

Neutral-current coupling in high-energy neutrino interactions

F. S. Merritt,* B. C. Barish, J. F. Bartlett, A. Bodek,[†] K. W. Brown, D. Buchholz,[‡] F. Jacquet,[§] F. J. Sciulli,
L. Stutte,[¶] and H. Suter^{||}

California Institute of Technology, Pasadena, California 91125

H. E. Fisk and G. Krafczyk

Fermi National Accelerator Laboratory, Batavia, Illinois 60510

(Received 14 November 1977)

We present measured hadron energy distributions for the reactions $\nu(\bar{\nu}) + N \rightarrow \nu(\bar{\nu}) + \text{hadrons}$ at high energy, as well as for the similar charged-current interactions. Insofar as possible, the determination of these distributions avoids any *a priori* assumptions about either the neutral-current or the charged-current interactions. We further analyze the neutral-current distributions within the framework of specific models, particularly the scaling model, to obtain a positive-helicity component $P = 0.36 \pm 0.10$, which lies between pure $V - A$ and pure V or A , and a coupling strength of $g_0 = 0.31 \pm 0.03$ relative to the charged-current interaction. These coupling parameters agree well with the predictions of the Weinberg-Salam model with $\sin^2\theta_w = 0.33 \pm 0.07$.

I. INTRODUCTION

This paper presents the results of an experiment to investigate the structure of the neutral-current coupling in the deep-inelastic interaction

$$\nu(\bar{\nu}) + N \rightarrow \nu(\bar{\nu}) + \text{hadrons}. \quad (1)$$

This process was predicted by gauge theories such as the Weinberg-Salam model,¹ and has since been observed in several experiments.²⁻⁴

Experimental results are usually described in terms of the ratios $R^\nu = \sigma_{\text{NC}}^\nu / \sigma_{\text{CC}}^\nu$ and $R^{\bar{\nu}} = \sigma_{\text{NC}}^{\bar{\nu}} / \sigma_{\text{CC}}^{\bar{\nu}}$. However, the scaling behavior of charged and neutral currents could be quite different (if, for example, the charged currents deviate from scaling by the production of new quarks). In order to keep the charged- and neutral-current processes distinct, in this paper we have endeavored to analyze the neutral-current events with as little dependence as possible on the form of the charged-current data.

The differential cross sections of process (1) can be written as

$$\frac{d\sigma}{dE_h} = \frac{G^2 M}{\pi} C_0 f(y, E_\nu), \quad \frac{d\bar{\sigma}}{dE_h} = \frac{G^2 M}{\pi} C_0 \bar{f}(y, E_{\bar{\nu}}), \quad (2)$$

where E_h = hadronic energy, E_ν = incident neutrino energy, M = nucleon mass, and G = Fermi constant, and C_0 is a constant related to the nucleon structure [$C_0 = \int F_2(x) dx$]. To the extent that the interaction scales, the functions f and \bar{f} are independent of E_ν . These inelasticity functions are the crucial measurements in that their forms and relative magnitudes reflect the Lorentz structure of the neutral current and their absolute magnitudes are determined by the strength of the neutral-current

coupling.

In Sec. II we describe the experimental procedure and the determination of these differential distributions (2). The distributions are extracted with minimal *a priori* assumptions about the physics of both charged-current (CC) and neutral-current (NC) interactions.

In Sec. III the data are compared to specific models of the neutrino interaction (primarily the scaling model with charged currents coupling through $V - A$ and neutral currents coupling through a combination of $V - A$ and $V + A$). Within this framework, the Weinberg angle and the fractional $V + A$ component of the NC coupling are determined. In addition, the constraints imposed on the data by assuming these forms reduce the statistical errors of Sec. II (but at the expense of model independence).

II. DETERMINATION OF THE DIFFERENTIAL DISTRIBUTIONS

The primary goal of this experiment was to provide measured values for the neutrino and antineutrino functions (2), with as little reliance as possible on *a priori* assumptions regarding the underlying mechanism. However, this goal is not easily achieved because in reaction (1) no incident particle can be directly seen, and only the outgoing hadronic system is observable. To accomplish it, certain independently determined information is necessary: principally, (1) knowledge of the incident neutrino energy and (2) good separation of neutrino and antineutrino interactions. These were provided here by the use of the Fermilab narrow-band neutrino beam,⁵ tuned in turn to positive and negative hadrons of mean energy 170 GeV. Figure 1 shows the calculated energy distributions nor-

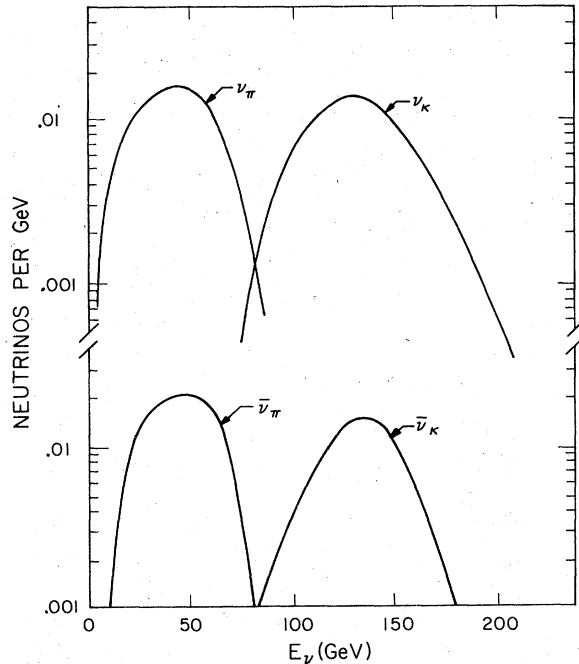


FIG. 1. Calculated flux vs energy incident onto the fiducial volume from the narrow-band neutrino and anti-neutrino beams. Included are neutrinos from decays of pions (ν_π) and kaons (ν_K) in the decay pipe. Each spectrum (e.g., ν_π) has been normalized to unit integral.

malized to unit area, for the neutrino fluxes incident onto the apparatus. These spectral shapes depend mainly on the optical settings of the beam and only secondarily on π/K production spectra by 300-GeV protons. The charged-current events taken simultaneously,⁶ in which all energy is measured, corroborate the shapes of these distributions.

Neutrinos originating upstream of the decay pipe present a serious background for the measurement of $\nu(\bar{\nu})$ induced neutral-current distributions. This "wide-band" component presents a special problem because it contains both neutrinos and antineutrinos. In addition, this spectrum, which is peaked at low energy, depends directly on uncertain details of hadronic production at the proton target. Because of these complications, we have measured this background directly and made a statistical subtraction from the data in each bin of hadron energy E_h . This was accomplished by running the experiment for approximately one-third of the data taking with the hadron beam absorbed just prior to the entrance of the decay pipe so that only wide-band events were produced during this time. The measured magnitude of this wide-band neutral-current background (8% for ν , 38% for $\bar{\nu}$) relative to the narrow-band neutral-current signal was

about twice the value estimated by thin target flux calculations.

Neutral-current events were collected in the Caltech-Fermilab detector⁵ simultaneously with charged-current events which have been described in a previous paper.⁶ An event was recorded whenever more than 12 GeV of hadron energy deposition was sensed in coincidence with the 1-msec beam spill. The separation of charged-current events ($\nu_\mu + N \rightarrow \mu^- + \text{hadrons}$) from neutral-current events was accomplished later by exploiting the difference in penetration in the steel target between the charged secondaries for a neutral-current event and a muon in a charged-current event. The technique was essentially identical to that utilized in a previous experiment by the authors.⁴ The raw neutral-current data sample consisted of those events wherein the most penetrating particle downstream of the interaction point traversed less than 1.6 m of steel. There were 1033 ν_μ events and 239 $\bar{\nu}_\mu$ events in this raw sample. The raw charged-current sample, with events of longer penetration, was retained as a control sample. This division retains some contamination of the neutral-current raw data from charged-current events in a limited kinematic range, i.e., those with muon angle greater than about 225 mrad and those with muon energy less than about 2.4 GeV. The subtraction of this charged-current remnant will be addressed in more detail later.

The raw data sample was first corrected for the measured wide-band background component (described previously) and for background triggers due to cosmic rays impinging on the apparatus simultaneously with the beam. The latter (7% for ν , 14% for $\bar{\nu}$) was also directly measured utilizing a second beam gate separated in time from the actual beam spill time. Other corrections, including those due to errors in determining the interaction point, penetration of high-energy showers past the 1.6-m cutoff, and interactions of electron type neutrinos were also made at this time. These latter (each amounting to less than 4% for both ν and $\bar{\nu}$) were considerably smaller effects than those from wide-band background or cosmic-ray contamination. The resulting data samples, it should be emphasized, are purely separated neutrino and antineutrino events from neutrinos of known mean energy within the statistical limitations of the various subtractions.

The problem of misidentified charged-current events is illustrated in Fig. 2. It shows the approximate acceptance (curve a) for recognizing a secondary muon from 60-GeV neutrino interactions using the penetration requirement described previously. This efficiency is plotted against the scaling variable y . The identification problem arises

primarily because muons of large polar angle (θ) exit the apparatus transversely before penetrating the minimum longitudinal distance. However, for muons with polar angle, θ , less than 300 mrad, the effect of this geometrical acceptance can be measured directly from the data by rotating the azimuthal angle ϕ of each recognized CC event through 2π , and calculating the fraction of "missed" muons with the same θ . This procedure, which assumes only that the cross section is independent of azimuth, statistically corrects for CC contamination with $\theta \leq 300$ mrad. The remaining CC background from events with $\theta_\mu > 300$ mrad (and predominantly $y > 0.9$) must be extrapolated, and this extrapolation depends on the form of the x and y distributions.

In a previous paper⁶ we have compared various models (e.g., scaling, nonscaling, b -quark production) to the CC data of this same experiment. Each of these models was used here to estimate the remaining CC background and its uncertainty. In order to minimize the dependence on the model, the background from wide-angle muons (above curve b in Fig. 2) was determined relative to the background from medium-angle muons (between curves a and b). Calculated in this way, the additional correction was very insensitive to the model, and amounted to an additional subtraction from the neutral-current sample of $(26.5 \pm 2.3)\%$ for neutrinos and $(11.5 \pm 3.5)\%$ for antineutrinos (amounting

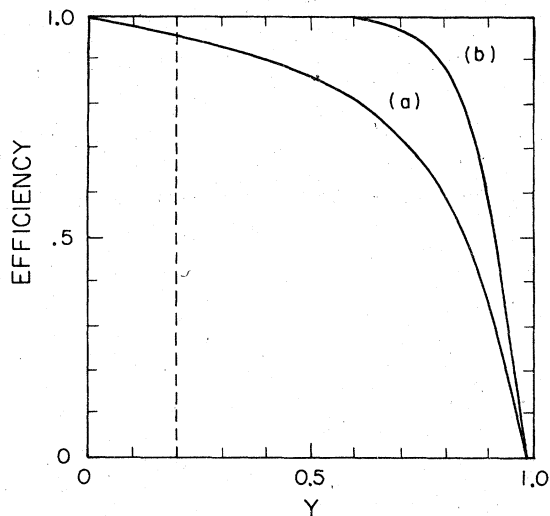


FIG. 2. Calculated efficiency for recognizing charged-current events induced by 60-GeV neutrinos. (a) All events with muon penetration greater than 1.6-m steel. (b) Events after correcting for losses measured by azimuthal rotation of recognized events (see text). The dashed line indicates the effect of the 12-GeV trigger requirement.

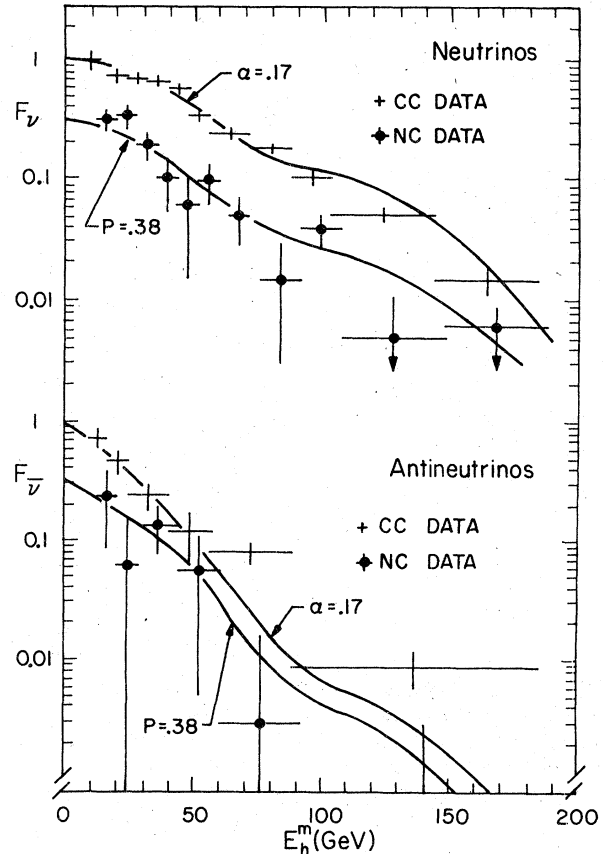


FIG. 3. The neutral-current and charged-current distributions in measured hadron energy using the model-independent techniques of azimuthal extrapolation for part of the charged-current subtraction and y intercepts for normalization. For comparison, the scaling-model curves for $\alpha = 0.17$ for the charged currents (Ref. 6), and $P = 0.38$ for the neutral currents (Ref. 7) are shown.

to about half the total correction in each case). The central values represent the result of the scaling model, and the errors are the systematic uncertainty determined by the full range covered by the other models (within the limits described in Refs. 6 and 7). The larger percentage effect for neutrino events reflects their larger charged-current cross section at large y . The larger error for antineutrino events reflects their greater theoretical and experimental uncertainty at large y .

The corrected hadron energy distributions for both neutral- and charged-current events are shown in Fig. 3. They are normalized to facilitate fits for $f(y)$, $\bar{f}(y)$ in Eq. (2). In the experiment, the flux was not measured independently, so we have chosen to normalize to charged-current data. The least controversial region of the charged-current cross section is at small values of hadron

energy, where the neutrino and antineutrino cross sections at the same energy are predicted by charge symmetry to be approximately equal. The hadron spectra for CC events were measured separately for pion and kaon neutrinos near $E_h = 0$ in this experiment with events from a separate (muon) trigger,⁶ and form the normalization used for Fig. 3. Therefore, the ordinate (F) represents the ratio

$$F(E_h^m) = \frac{d\sigma^{\text{NC}}}{dE_h} \bigg/ \left(\frac{d\sigma^{\text{CC}}}{dE_h} \bigg|_{E_h^m=0} \right).$$

The experimental distributions of Fig. 3 get contributions from pion and kaon neutrinos $F(E_h^m) = F_\pi(E_h^m) + F_K(E_h^m)$ where, for example, for pion neutrinos,

$$F_\pi(E_h^m) = a_\pi \int \rho_\pi(E_\nu) dE_\nu \int R(E_h^m, E_h) f(E_h/E_\nu) dE_h,$$

a_π is the relative contribution to charged currents at $E_h = 0$ from pion neutrinos, ρ_π is the flux distribution shown in Fig. 1, and $R(E_h^m, E_h)$ is the resolution function for hadron energy measurement.⁸ The functions f and \bar{f} represent the physics functions of Eq. (2). The relative contributions to $F(E_h^m)$ from ν_π/ν_K are $a_\pi/a_K = 0.856/0.144$ for neutrinos and $0.966/0.034$ for antineutrinos. The overall relative ν - $\bar{\nu}$ uncertainty in the normalization is about 15%. The curves through the charged-current (control) samples are calculated from the scaling model of Ref. 6. The neutral-current data lie systematically below the charged-current data, reflecting a coupling constant smaller than the charged-current coupling by about a factor of 3.

Assumptions about the charged-current data have entered into this analysis at only two significant points: (1) in the small extrapolation of the charged-current background in the low E_h region, and (2) in the normalization of the fluxes using the y intercepts of the CC distributions. These are the minimal CC assumptions needed to obtain normalized NC distributions. Additional assumptions about the specific form of the NC interaction were not used at all in the analysis. The resulting distributions are therefore as model independent as possible.

In order to parameterize these distributions in a simple way, we will now assume that the neutral current couples through some combination of V and A . In this case, the inelasticity function (2) should be of the form

$$\begin{aligned} f(y) &= g_0[(1-P) + P(1-y)^2], \\ \bar{f}(y) &= g_0[(1-P) + (1-y)^2 + P], \end{aligned} \quad (3)$$

where P is a constant representing the fractional amount of positive-helicity coupling (P receives contributions from V - A coupling to antiquarks as

well as from V + A coupling to quarks). Using the flux distributions of Fig. 1, with normalization determined by the y intercepts of the CC data, the neutral-current distributions can be fitted to give both P and the normalization,

$$\begin{aligned} P &= 0.38 \pm 0.13, \\ g_0 &= 0.32 \pm 0.05. \end{aligned} \quad (4)$$

The corresponding curves⁹ are compared to the NC data in the figure.

III. DETERMINATION OF THE V + A AND V - A STRUCTURE OF THE COUPLING

The preceding section analyzed the neutral-current data on very general grounds. In this section, we use specific models of the charged-current interaction (primarily the scaling model) to extend that analysis. Using the antiquark component determined from the CC data, the V + A and V - A components of the neutral-current coupling will be determined and compared to various models of the neutral-current coupling.

The additional constraints imposed by using a specific charged-current model allow a more precise determination of the CC background and of the relative ν and $\bar{\nu}$ fluxes, and consequently of the neutral-current couplings. The validity of the results, of course, is limited to some extent by the validity of the model.

In the usual scaling model of the charged-current interaction, the coupling is assumed to be V - A and the distributions are

$$\frac{d\sigma^\nu}{dy}(\text{CC}) = \bar{E}[(1-\alpha) + \alpha(1-y)^2], \quad (5a)$$

$$\frac{d\sigma^{\bar{\nu}}}{dy}(\text{CC}) = \bar{E}[\alpha + (1-\alpha)(1-y)^2], \quad (5b)$$

where $\bar{E} = (G^2ME/\pi) \int_0^1 F_2(x) dx$. The shapes of the y distributions and the relative magnitudes of the total cross section are determined by the parameter α , interpreted as the antiquark component in the nucleon. (In another common notation, $2\alpha = 1 - B$.) Dominantly flat distributions for ν events and $(1-y)^2$ distributions for $\bar{\nu}$ events are consequences of V - A coupling and the dominant negative helicities of the interacting nucleon constituents (e.g., quarks). The charged-current data reported previously from this experiment⁶ yield a best value of $\alpha = 0.17 \pm 0.12$.

Predictions of gauge theories, as well as the analogy to charged- and electromagnetic-current couplings, suggest that the neutral current also couples through a combination of V and A . For most of the analysis reported in this paper, we have assumed a V , A type coupling for the neutral

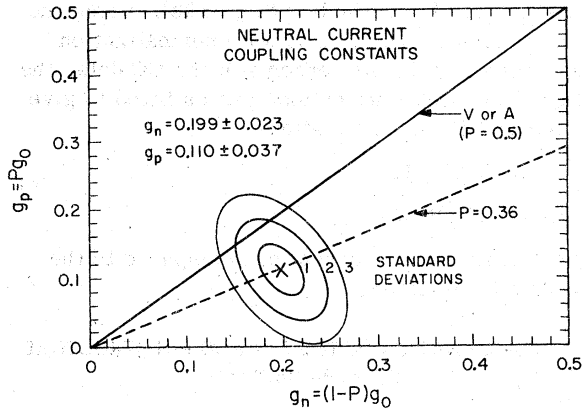


FIG. 4. The negative- (g_n) and positive-helicity (g_p) coupling parameters, obtained by fitting the neutral-current E_h distributions, define a point in the plot. The elliptical curves surrounding the point indicate the 1, 2, and 3 standard deviation limits due to statistical error. The result is about 3σ from pure negative helicity and 1.5σ from pure V or A .

current and under this assumption, the neutral-current distributions are similar in form to the charged-current distributions above,

$$\frac{d\sigma^\nu}{dy}(\text{NC}) = \bar{E}g_0[(1-P) + P(1-y)^2], \quad (6a)$$

$$\frac{d\sigma^{\bar{\nu}}}{dy}(\text{NC}) = \bar{E}g_0[P + (1-P)(1-y)^2]. \quad (6b)$$

P , analogous to α in equations (5a) and (5b), is a "positive-helicity" parameter. However, in this case it receives contributions from both (a) $V-A$ coupling to the antiquark component in the nucleon and (b) $V+A$ coupling to the quark component. The structure of the neutral-current coupling affects only P , while the strength of the coupling determines g_0 (measured relative to the usual charged-current coupling). In the event that neutral currents and charged currents scatter from the same nucleon components, we can make some direct predictions. If the neutral-current coupling is pure $V-A$ (like the charged current), $P = \alpha$, and if the coupling is pure V or pure A , $P = \frac{1}{2}$. (The last statement is independent of the nucleon constituents.)

In order to determine P and g_0 within the framework of a scaling model, we first used Eqs. (5a) and (5b) to fit the distributions of CC events with a visible muon (see Ref. 6). This immediately provides the relative flux normalizations of ν and $\bar{\nu}$. It also determines, by extrapolation, the background of wide-angle and low-energy CC events in the sample with no visible muon.

After correcting for this background, the neu-

tral-current distributions were fitted with the form of Eqs. (6a) and (6b) including the relative normalizations, to determine g_0 and P . Figure 4 shows the results of this two-parameter fit. The 1, 2, and 3 standard deviation contours for this fit are shown in the figure. The best values for the parameters are $g_0 = 0.31 \pm 0.02$ and $P = 0.36 \pm 0.09$. This value for P is about three standard deviations from pure negative-helicity scattering and about 1.5 standard deviations from pure V or pure A .

Using these fitted parameters, the hadron distributions measured for $E_h \geq 12$ GeV were extrapolated to $E_h = 0$ in order to obtain the total cross-section ratios. This extrapolation yields

$$\frac{\sigma^\nu(\text{NC})}{\sigma^\nu(\text{CC})} = 0.27 \pm 0.02,$$

$$\frac{\sigma^{\bar{\nu}}(\text{NC})}{\sigma^{\bar{\nu}}(\text{CC})} = 0.40 \pm 0.08, \quad (7)$$

and

$$\frac{\sigma^{\bar{\nu}}(\text{NC})}{\sigma^\nu(\text{NC})} = 0.75 \pm 0.15.$$

The cross sections $\sigma^{\bar{\nu}}(\text{NC})$ and $\sigma^\nu(\text{NC})$ are expected to be equal in some vectorlike theories.¹⁰ Our results, while not completely inconsistent, do not favor this possibility.

The physics of charged currents only affects the determination of the neutral-current coupling parameters through (1) the calculated neutrino-anti-neutrino flux ratio, and (2) the calculated CC contamination in the neutral-current signal. We have tested the sensitivity of the neutral-current analysis to the assumed form of the charged-current distributions by allowing α to vary over the range (0.11–0.29) allowed by the charged-current data, and we have also used models incorporating an energy-dependent α , production of new heavy quarks, and varying x distribution.⁷ All models which were consistent with the charged-current data reproduced the values of g_0 and P to within approximately one-half of a statistical standard deviation. With all of these variations taken into account, the neutral-current coupling parameters from these data are

$$g_0 = (0.31 \pm 0.02) \pm 0.02$$

and

$$P = (0.36 \pm 0.04) \pm 0.09, \quad (8)$$

where the inner errors are due to the systematic (model-dependent) variations and the outer errors are statistical.

Extracting the amount of $V-A$ and $V+A$ coupling for the neutral currents is by necessity more model dependent than the above analysis, since the

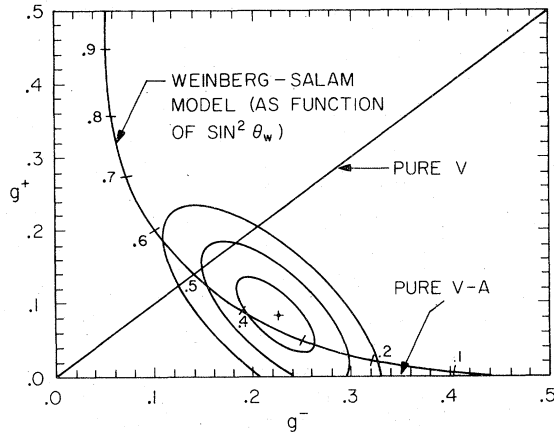


FIG. 5. A plot of the $V-A$ and $V+A$ coupling parameters g^- and g^+ is shown. A value of $\alpha=0.17$ for the antiquark component has been used. For comparison, the prediction of the Weinberg-Salam model is shown with values of $\sin^2\theta_w$ as indicated.

separation depends on the antiquark fraction in neutral currents. We have determined these coupling parameters by using the neutral-current parameters g_0 and P determined above, with the value of α determined from the charged-current data. The relations between these parameters are

$$g_n = (1 - P)g_0 = (1 - \alpha)g^- + \alpha g^+ \quad (9)$$

and

$$g_p = P g_0 = (1 - \alpha)g^+ + \alpha g^-,$$

where g^- and g^+ are the absolute magnitudes of the neutral-current $V-A$ and $V+A$ coupling strengths, respectively. The Weinberg-Salam model¹ can be directly compared with results presented in this form since the positive-helicity contribution from the antiquark component of the struck nucleon has been removed. In the Weinberg-Salam model, these couplings can be expressed in terms of a single parameter $\sin^2\theta_w$ as follows:

$$g^- = \frac{1}{2} - \sin^2\theta_w + \frac{5}{9} \sin^4\theta_w \quad (10)$$

and

$$g^+ = \frac{5}{9} \sin^4\theta_w,$$

neglecting small effects of the Cabibbo angle, etc. Figure 5 shows this curve in the g^- vs g^+ plane along with the results for the neutral-current parameters from this experiment, using $\alpha=0.17$.

The data agree with the Weinberg-Salam model in magnitude and yield a best fit

$$\sin^2\theta_w = 0.33 \pm 0.07. \quad (11)$$

More generally, scalar, pseudoscalar, and tensor couplings could, in principle, contribute to the neutral-current signal. In an extreme case, pure scalar or pseudoscalar couplings would produce $d\sigma/dy \propto y^2$ distribution for both ν and $\bar{\nu}$. This is inconsistent with both the shapes and the relative magnitude of the measured hadron energy distributions, and is ruled out at the level of 5 standard deviations.

In the most general case, Eqs. (6a) and (6b) may each contain an additional term of the form $C(1-y)$. A three-parameter fit to the data in fact gives a large C component. However, the two-parameter V and A fit is also consistent with the data and yields a similar χ^2 . We, therefore, have no compelling evidence for a $(1-y)$ term, but are unable to exclude it.

Since the data involved two different energies, we can make a crude comparison to test for Z^0 propagator effects. We observe no such energy-dependent effects. Internally to these data we place a limit of $M_{Z^0} > 3$ GeV at the 90% confidence level. A better limit can be obtained by comparing with data at much lower energy.^{2,7}

In conclusion, the neutral-current hadron energy distributions are consistent with a combination of V and A couplings. The coupling appears to lie approximately midway between V or A and $V-A$, and about 1.5–2 standard deviations from each. These couplings agree quite well with the predictions of the Weinberg-Salam theory, and require a Weinberg angle consistent with the values obtained from other experiments.^{2,11}

ACKNOWLEDGMENTS

We wish to thank the Fermilab staff for their contributions to this experiment. In particular, we are indebted to Helen Edwards and the beam-extraction group for developing the fast-spill resonant extraction used in this experiment, and to the Neutrino Lab for their continuing help and cooperation. This work was supported by the U.S. Department of Energy, prepared under Contract No. EY-76-C03-0068 for the San Francisco Operations Office.

*Present address: Stanford University, Stanford, California 94305.

†Present address: University of Rochester, Rochester, New York 14627.

‡Present address: Northwestern University, Evanston, Illinois 60201.

§Present address: Ecolé Polytechnique, Paris, France.

¶Present address: Fermi National Accelerator Labora-

tory, Batavia, Illinois 60510.

||Present address: CERN, Geneva 23, Switzerland.

¹S. Weinberg, *Phys. Rev. Lett.* **19**, 1264 (1967);

A. Salam, *Elementary Particle Theory: Relativistic Groups and Analyticity (Nobel Symposium No. 8)*, edited by N. Svartholm (Almqvist and Wiksell, Stockholm, 1968), p. 367.

²F. J. Hasert *et al.*, *Phys. Lett.* **46B**, 138 (1973); F. J. Hasert *et al.*, *Nucl. Phys.* **B73**, 1 (1974).

³A. Benvenuti *et al.*, *Phys. Rev. Lett.* **32**, 800 (1974).

⁴B. C. Barish *et al.*, *Phys. Rev. Lett.* **34**, 538 (1975).

⁵B. C. Barish *et al.*, Fermilab Report No. 21, 1970 (unpublished); P. Limon *et al.*, *Nucl. Instrum. Methods* **116**, 317 (1974).

⁶B. C. Barish *et al.*, *Phys. Rev. Lett.* **38**, 314 (1977).

⁷F. Merritt, Ph.D. thesis, Caltech, 1976 (unpublished).

⁸The resolution function used was of a Gaussian form $dR(E_h, E_h^m) = 1/(2\pi\sigma^2)^{1/2} \exp[-(E_h - E_h^m)^2/2\sigma^2] dE_h^m$, and $\sigma = 1.1\sqrt{E_h}$ (energy units are GeV).

⁹The NC/CC ratios of $R^\nu = 0.27$ and $R^{\bar{\nu}} = 0.42$ can be cal-

culated from these parameters and the analogous CC parameters (we assume $\alpha = 0.17$ and $g_0 = 1$ for CC events). For comparison, the ratios of the raw data in Fig. 3 for $E_h > 12$ GeV are $R^\nu = 0.28 \pm 0.03$ and $R^{\bar{\nu}} = 0.35 \pm 0.11$. The change in $R^{\bar{\nu}}$ is due primarily to the importance of the flux normalization (obtained from the CC γ intercepts) and of the shape and normalization constraints imposed by assuming (6) for the neutral currents, rather than to the extrapolation to $E_h = 0$.

¹⁰A. De Rújula *et al.*, *Phys. Rev. D* **12**, 3589 (1975); R. L. Kingsley *et al.*, *ibid.* **12**, 2768 (1975); H. Fritzsch *et al.*, *Phys. Lett.* **59B**, 256 (1975); S. Pakvasa *et al.*, *ibid.* **35**, 703 (1975).

¹¹M. Holder *et al.*, CERN report, 1977 (unpublished). They have obtained a value $\sin^2\theta_w = 0.24 \pm 0.02$, without applying the normalization constraint required here. Our central value would be in closer agreement if we relaxed that requirement.